Pyrazine-Derived Disulfide-Reducing Agent for Chemical Biology

John C. Lukesh, III, Kelly K. Wallin, and Ronald T. Raines*

Contents

I. General

Commercial reagents were used without further purification. Dithiothreitol (DTT) was from Research Products International (Mt. Prospect, IL). *N*,*N*′-dimethylhydrazine dihydrochloride was from Santa Cruz Biotechnology, Inc (Dallas,TX). Papain (lyophilized powder from papaya latex), creatine kinase (lyophilized powder from rabbit muscle), hexokinase (lyophilized powder from *Saccharomyces cerevisiae*), glucose-6-phosphate dehydrogenase (ammonium sulfate suspension from baker's yeast), N_α-benzoyl-L-arginine-4-nitroanilide hydrochloride, *S*-methyl methanethiosulfonate, *trans*-4,5-dihydroxy-1,2-dithiane (oxidized DTT), 2-mercaptoethanol, oxidized 2-mercaptoethanol, and 2-butyne-1,4-diol were from Sigma–Aldrich (St. Louis, MO). DTBA and oxidized DTBA were synthesized as described previously.[1]

All glassware was oven or flame-dried, and reactions were performed under N_2(g) unless stated otherwise. Dichloromethane was dried over a column of alumina. Triethylamine and dimethylformamide (DMF) were dried over a column of alumina and purified further by passage through an isocyanate scrubbing column. Flash chromatography was performed with columns of 40−63 Å silica, 230−400 mesh (Silicycle, Québec City, Canada). Thin-layer chromatography (TLC) was performed on plates of EMD 250-um silica 60-F_{254}. The term "concentrated under reduced pressure" refers to the removal of solvents and other volatile materials using a rotary evaporator at water-aspirator pressure (<20 torr) while maintaining the water-bath temperature below 40 °C. Residual solvent was removed from samples at high vacuum (<0.1 torr). The term "high vacuum" refers to vacuum achieved by a mechanical belt-drive oil pump. Analytical

samples of BMMP and BMMP^{ox} were obtained using a Shimadzu (Kyoto, Japan) preparative HPLC, equipped with a C18 reverse-phase preparative column, Prominence diode array detector, and fraction collector. Ellman's assay for sulfhydryl groups was performed using a Varian Cary 60 Bio UV–Vis spectrophotometer. Equilibrium, reduction potential, and kinetic studies on small molecules were performed with an analytical HPLC (Waters system equipped with a Waters 996 photodiode array detector, Empower 2 software and a Varian C18 reverse-phase column). Thiol pK_a values were determined using a Varian Cary 60 UV–Vis spectrophotometer. Kinetic studies on proteins were carried out using a Varian Cary 400 Bio UV–Vis spectrometer with a Cary temperature controller at the Biophysics Instrumentation Facility at Madison (BIF). All NMR spectra were acquired at ambient temperature with a Bruker DMX-400 Avance spectrometer and a Bruker Avance III 500ii with cyroprobe spectrometer at the National Magnetic Resonance Facility at Madison (NMRFAM), and were referenced to TMS or residual protic solvent.

II. Computational procedures

Idealized conformations of **4**, **5**, DMH, DMH^{ox}, DTT, and DTT^{ox} were determined by optimizing their geometries at the B3LYP/6-311+G(2d,p) level of theory as implemented by Gaussian 09.[2] The optimized structures yielded no imaginary frequencies, indicating a true energy minimum on the potential energy surface.

III. Chemical synthesis

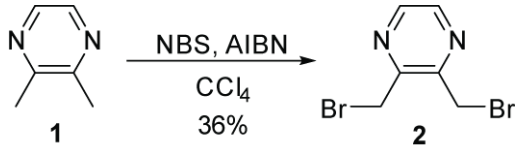

Compound **2** was synthesized as described previously from 2,3-dimethylpyrazine (**1**) resulting in comparable yields and identical NMR spectra.[3]

^{1}H NMR (400 MHz, $CDCl_3$) δ = 8.43 (s, 2H), 4.65 (s, 4H); **^{13}C NMR (125 MHz, $CDCl_3$)** = 151.4, 143.9, 29.5.

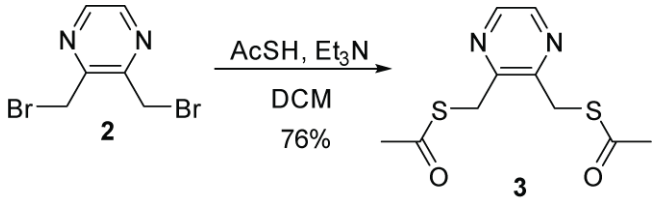

A flame-dried round-bottom flask was charged with **2** (0.907 g, 3.411 mmol), dissolved with 35 mL of dichloromethane, and placed under an atmosphere of dry N_2(g). Triethylamine

(1.50 mL, 10.76 mmol) and thioacetic acid (0.54 mL, 7.56 mmol) were then added, and the resulting solution was stirred overnight. After 16 h, the reaction was concentrated under reduced pressure and the resulting residue was purified by column chromatography (40% v/v ethyl acetate in hexanes) resulting in **3** (0.664 g, 76%).

^{1}H NMR (400 MHz, $CDCl_3$) δ = 8.42 (s, 2H), 4.43 (s, 4H), 2.39 (s, 6H); **^{13}C NMR (100 MHz, $CDCl_3$)** δ = 194.4, 151.1, 142.8, 32.4, 30.2; **HRMS** (ESI) calculated for $[C_{10}H_{13}N_2O_2S_2]^+$ ($M+H^+$) requires m/z = 257.0413, found 257.0422.

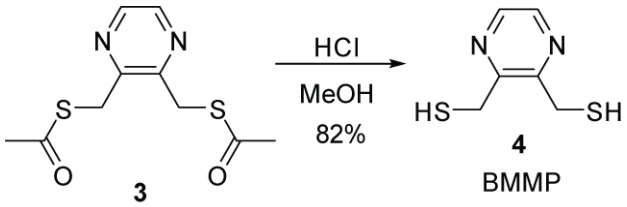

To a flame-dried flask containing **3** (0.167 g, 0.651 mmol) was added 6 mL of anhydrous MeOH followed by 3 mL of 3 N HCl in MeOH. After reacting for 16 h under N_2(g), the reaction mixture was concentrated under reduced pressure, passed through a 4.5-µm filter, and purified by reverse-phase HPLC using a preparatory C18 column and a linear gradient of 10–80% v/v acetonitrile (0.1% v/v TFA) in water (0.1% v/v TFA) over 45 min. BMMP eluted at 27 min and, after lyophilization, was isolated as an off white/yellow powder (91.9 mg, 82%).

^{1}H NMR (400 MHz, DMSO-d_6) δ = 8.46 (s, 2H), 3.97 (d, J = 7.5 Hz, 4H), 3.05 (t, J = 7.5 Hz, 2H); **^{13}C NMR (100 MHz, DMSO-d_6)** δ = 153.3, 142.5, 26.8; **HRMS** (EI) calculated for $[C_6H_8N_2S_2]^+$ (M^+) requires m/z = 172.0124, found 172.0125.

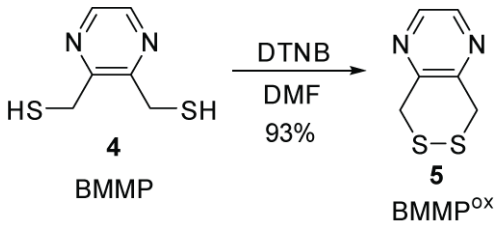

BMMP (51.5 mg, 0.299 mmol) and 5,5′-dithio-bis(2-nitrobenzoic acid) (118.9 mg, 0.300 mmol) were placed in a 25-mL round-bottom flask. These solids were dissolved in 7 mL of anhydrous DMF, and the reaction mixture was stirred under N_2(g). After 24 h, the solvent was removed by rotary evaporation under high vacuum, passed through a 4.5-µm filter, and purified by reverse-phase HPLC using a preparatory C18 column and a linear gradient of 10–80% v/v acetonitrile

(0.1% v/v TFA) in water (0.1% v/v TFA) over 45 min. BMMP^{ox} eluted at 36 min, and after lyophilization, was isolated as an off white/yellow powder (47.3 mg, 93%).

^{1}H NMR (400 MHz, $CDCl_3$) δ = 8.42 (s, 2H), 4.25 (s, 4H); **^{13}C NMR (100 MHz, $CDCl_3$)** δ = 149.8, 142.2, 37.9; **HRMS** (EI) calculated for $[C_6H_6N_2S_2]^+$ (M^+) requires m/z = 169.9967, found 169.9961.

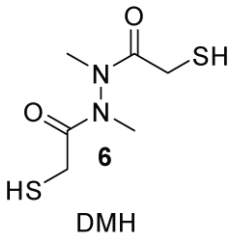

DMH

DMH was synthesized from *N*,*N*′-dimethylhydrazine dihydrochloride as described previously.[4] An analytically pure sample of **6** was obtained from reverse-phase HPLC using a preparatory C18 column and a linear gradient of 10–80% v/v acetonitrile (0.1% v/v TFA) in water (0.1% v/v TFA) over 45 min. DMH eluted at 23 min and, after lyophilization, was isolated as a white solid.

^{1}H NMR (400 MHz, Methanol-d_4) (Two unresolved conformations present[4]): δ = 3.53−3.21 (m), 3.08 (s); **^{13}C NMR (100 MHz, Methanol-d_4) (Two conformations present)** δ = 174.5, 174.4, 172.2, 38.1, 34.8, 32.7, 26.3, 25.5, 25.4; **HRMS** (ESI) calculated for $[C_6H_{13}N_2S_2]^+$ (M + H^+) requires m/z = 209.0413, found 209.0410.

IV. Determination of thiol pK_a values for BMMP

The thiol pK_a values for BMMP were determined by following closely a procedure reported previously that exploits the elevated absorbance of the deprotonated thiolate at 238 nm.[1, 5, 6] A plot of A_{238} *vs* pH was recorded (Fig. S1), and pK_a values were determined by fitting these data to eq 1, which is derived from both Beer's law and the definition of the acid dissociation constant.[5]

$$A_{238} = C_T\left(\frac{\varepsilon_{S^-}^{S^-}10^{(pH-pKa2)}+\varepsilon_{SH}^{S^-}+\varepsilon_{SH}^{SH}10^{(pKa1-pH)}}{10^{(pH-pKa2)}+1+10^{(pKa1-pH)}}\right) \quad (1)$$

In eq 1, C_T is the total thiol concentration, ε_{SH}^{SH} is the extinction coefficient of the doubly protonated form of BMMP, $\varepsilon_{SH}^{S^-}$ is the extinction coefficient of the singly protonated form of BMMP, and $\varepsilon_{S^-}^{S^-}$ is the extinction coefficient of the doubly deprotonated form of BMMP.

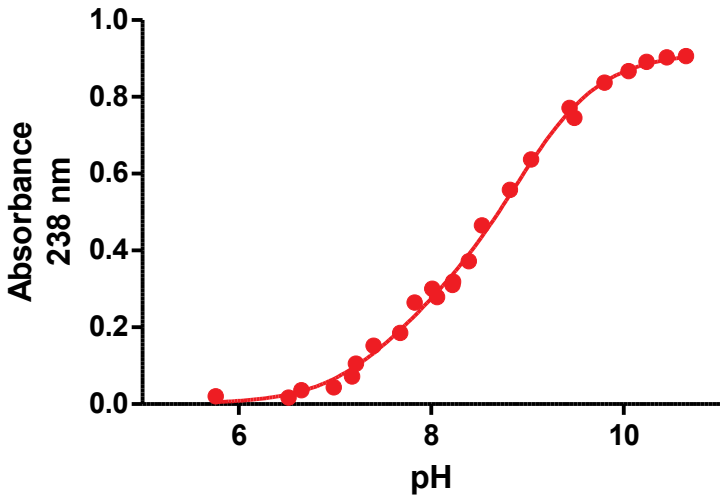

Fig. S1 Effect of pH on absorbance by BMMP at 238 nm in a 0.10 M potassium phosphate buffer. pK_a values of 7.6 ± 0.1 and 9.0 ± 0.1, and extinction coefficients of ε_{SH}^{SH} = 5.24, ε_{SH}^{S-} = 3058, ε_{S-}^{S-} = 9159 $M^{-1}cm^{-1}$ with $r^2 > 0.99$ were determined by fitting the data to eq 1.

V. Determination of thiol pK_a values for DMH

The thiol pK_as of DMH were also examined using the same conditions described above.

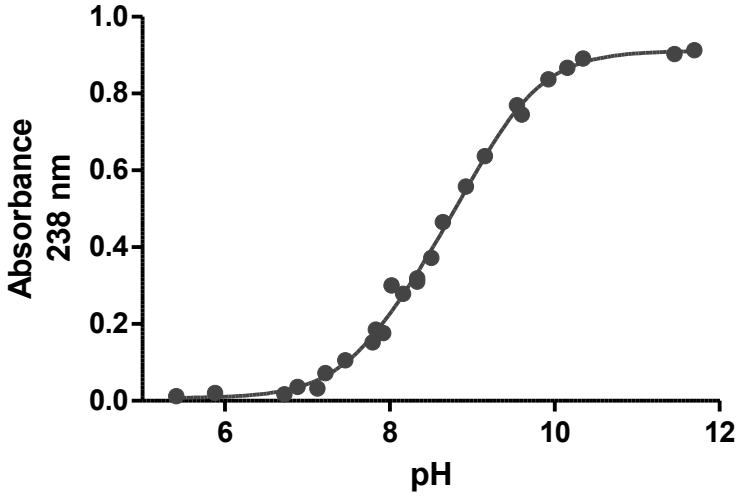

Fig. S2 Effect of pH on absorbance by DMH at 238 nm in a 0.10 M potassium phosphate buffer. pK_a values of 8.0 ± 0.2 and 9.1 ± 0.1, and extinction coefficients of ε_{SH}^{SH} = 67.8, ε_{SH}^{S-} = 3885, ε_{S-}^{S-} = 9116 $M^{-1}cm^{-1}$ with $r^2 > 0.99$ were determined by fitting the data to eq 1.

VI. Reduction potential of BMMP

Following a procedure reported previously,[1, 7] the reduction potential of BMMP was determined by analyzing its equilibrium reaction with DTT^{ox} (eq 2), and measuring the amount of reduced and oxidized species in solution by analytical HPLC. Once the equilibrium constant was

determined, its value was plugged into a variation of the Nernst equation (eq 3).[5] BMMP (2.5 mg, 0.015 mmol) and DTT^{ox} (2.3 mg, 0.015 mmol) were place in a 10 mL round-bottom flask, and 5 mL of degassed 50 mM potassium phosphate buffer, pH 7.0, containing EDTA (2 mM) was added. The reaction mixture was then sonicated briefly to ensure complete dissolution of material and stirred overnight under N_2(g). After reacting for 24 h, the reaction mixture was quenched by the addition of 0.1 mL of 3 N HCl, and passed through a 4.50-μm filter. A 100-μL aliquot of the reaction mixture was then immediately analyzed by analytical HPLC using a Waters system equipped with a Waters 996 photodiode array detector, Empower 2 software, and a Varian C18 column. The column was eluted at 1.0 mL/min with water (5.0 mL), followed by a linear gradient (0–40% v/v) of acetonitrile/water over 40 min. Four peaks were observed, corresponding to DTT (18 min), DTT^{ox} (22 min), BMMP (34 min), and $BMMP^{ox}$ (41 min) (Fig. S3). Calibration curves were generated and found to be linear over the concentration range analyzed. From these curves, equilibrium concentrations were determined, and a $K_{eq} = 0.137 \pm 0.036$ was determined for the reaction. Next, using this value and assuming $E^{\circ\prime} = -0.327$ V for DTT, a variation of the Nernst equation (eq 3) was used to calculate that BMMP has a reduction potential of $E^{\circ\prime} = (-0.301 \pm 0.003)$ V. This value is the mean ± SE from three separate experiments.

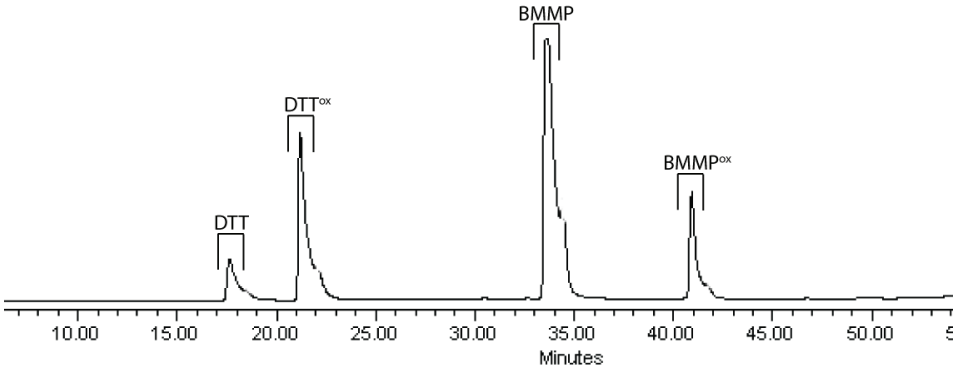

Fig. S3 Representative HPLC chromatogram of the redox equilibrium between BMMP and DTT^{ox}. Compounds were detected by their absorbance at 205 nm.

$$K_{eq} = \frac{[\text{DTT}][\text{oxidized BMMP}]}{[\text{BMMP}][\text{oxidized DTT}]} \tag{2}$$

$$E_{\text{BMMP}}{}^{\circ\prime} = E_{\text{DTT}}{}^{\circ\prime} - \frac{RT}{nF} \ln \frac{[\text{DTT}][\text{oxidized BMMP}]}{[\text{BMMP}][\text{oxidized DTT}]} \tag{3}$$

VII. Reduction Potential of DMH

The reduction potential of DMH was also determined by following the same procedure described in Section V. With $K_{eq} = 0.0065 \pm 0.0020$ and assuming $E^{\circ\prime} = -0.327$ V for DTT, DMH was found to have $E^{\circ\prime} = (-0.262 \pm 0.004)$ V.

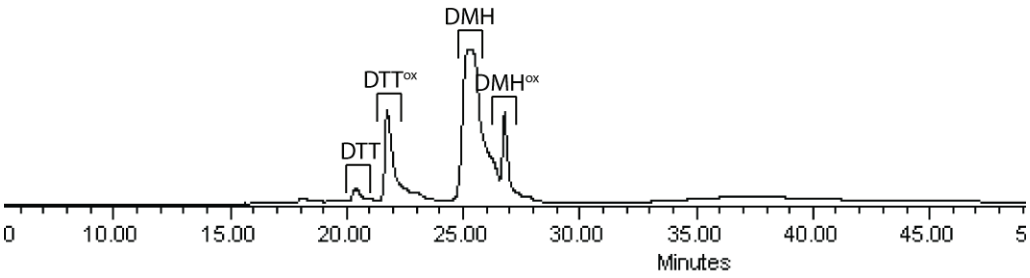

Fig. S4 Representative HPLC chromatogram of the redox equilibrium between DMH and DTT^{ox}. Compounds were detected by their absorbance at 205 nm.

VIII. Equilibrium reaction with oxidized βME

First, 4.0 mL of freshly degassed 50 mM potassium phosphate buffer, pH 7.0, containing EDTA (2 mM) was added to a round-bottom flask containing 3.0 mg (0.017 mmol) of BMMP. The flask was briefly sonicated to ensure complete dissolution of material and then stirred on under N_2(g). Next, 0.6 mL (0.006 mmol) of a 10 mM stock solution of βME^{ox} was added and the reaction was stirred overnight. After 24 h, the reaction mixture was quenched by the addition of 0.1 mL of 3 N HCl, filtered through a 4.5-µm solution, and immediately analyzed by analytical HPLC using a Waters system equipped with a Waters 996 photodiode array detector, Empower 2 software, and a Varian C18 column. The column was eluted at 1.0 mL/min with water (5.0 mL), followed by a linear gradient (0–40% v/v) of acetonitrile/water over 40 min. Three peaks were observed, corresponding to βME (6 min), BMMP (34 min), and $BMMP^{ox}$ (41 min). The peak corresponding to βME^{ox} (21 min) was not observed, indicative of the quantitative reduction of βME^{ox} to form βME (Fig. S5). This experiment was repeated three times with identical results.

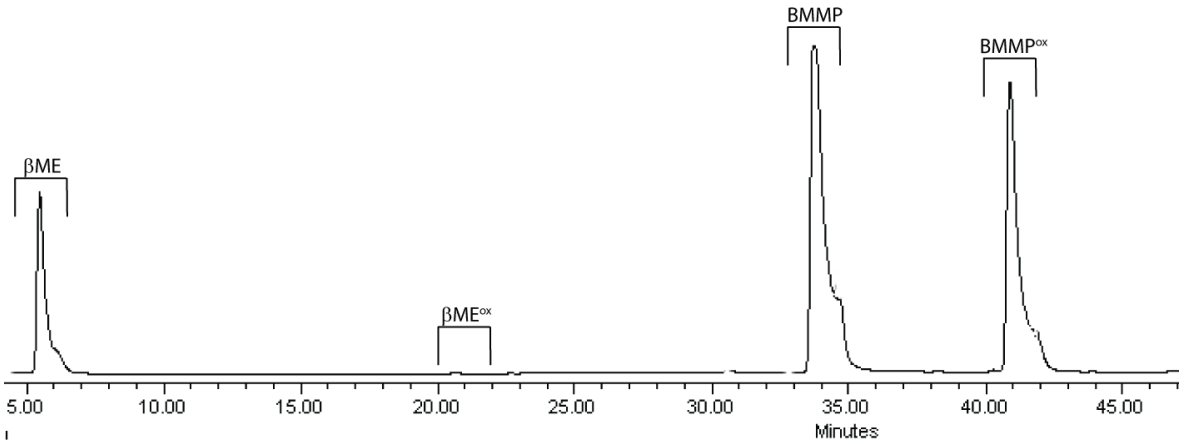

Fig. S5 Representative HPLC chromatogram of the redox equilibrium between BMMP and βME. Compounds were detected by their absorbance at 205 nm.

IX. Reduction kinetics on oxidized βME

$$-\frac{\partial[\text{disulfide}]_{\text{total}}}{\partial t} = k_{\text{obs}}[\text{disulfide}]_{\text{total}}[\text{thiol}]_{\text{total}}$$

The observed second-order rate constant (k_{obs}) for the reduction oxidized βME by BMMP, DMH, DTBA, and DTT was determined by following a previously described procedure.[1, 4] A 10 mL round-bottom flask was charged with BMMP (4.3 mg, 0.025 mmol), DTBA (4.3, 0.025 mmol), or DTT (3.9 mg, 0.025 mmol). Under an atmosphere of N_2(g), 2.5 mL of freshly degassed 50 mM potassium phosphate buffer, pH 7.0, was then added to the reaction flask and the solution was briefly sonicated to ensure complete dissolution of reducing agent. At time $t = 0$, 2.5 mL of a 10 mM stock solution of βME^{ox} in 50 mM potassium phosphate buffer, pH 7.0, was then added. At various time points (1, 2, and 4 min), the reaction mixture was quenched by the addition of 0.1 mL of 3 N HCl. The reaction mixture was then passed through a 4.5-μm filter and analyzed immediately by analytical HPLC using a Varian C18 reverse-phase column. The mixture was eluted at 1.0 mL/min with water (5.0 mL), followed by a linear gradient (0−40% v/v) of acetonitrile/water over 40 min. The degree of reduction was determined by integrating the newly formed peak in the chromatogram corresponding to reduced βME (elution time of 6 min) at 205 nm. Calibration curves were generated and determined to be linear over the concentration range. The amount of residual oxidized BME was calculated, and the second-order rate constants were determined from the linear fit of the data in Fig. 1A ($k_{\text{obs}} = [(1/C_{\text{final}}) - (1/C_{\text{initial}})]/t$). The initial values of concentration (C_{initial}) were: BMMP, DMH, DTBA, or DTT = βME^{ox} = 5 mM. Values of k_{obs} (Table S1) are the mean ± SE from three independent experiments. The same procedure was repeated with BMMP, DTBA, and DTT in 50 mM sodium acetate buffer, pH 5.0.

X. Reactivation of papain

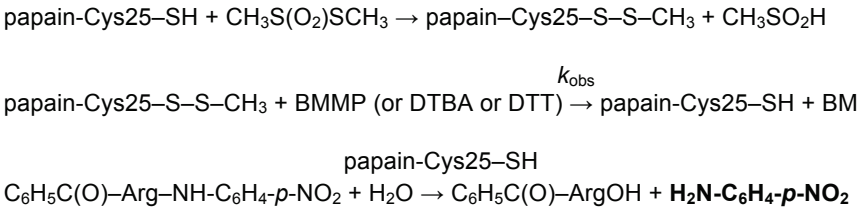

Papain was inactivated by forming a mixed disulfide upon treatment of its active-site cysteine (Cys25) with *S*-methyl methanethiosulfonate following a procedure reported previously.[1,8] A 1.25 mL solution of papain-Cys25−S−S−CH_3 (4.4×10^{-6} M) in a degassed 0.10 M imidazole−HCl buffer, pH 7.0, containing EDTA (2 mM) was placed in a 1.5-mL LoBind Eppendorf tube. At time $t = 0$, 10 μL of a 1 mM stock solution of BMMP was added, and a timer was started. The initial concentrations of the reaction mixture were dithiol reducing agent: 7.9×10^{-6} M and inactive protein: 4.4×10^{-6} M. At various time points, a 200-μL aliquot of the reaction mixture

was removed and added to a cuvette containing 800 μL of substrate solution (0.10 M imidazole–HCl buffer, pH 6.0, containing 2 mM EDTA and 1.25 mM *N*-benzoyl-L-arginyl-*p*-nitroanilide), and the rate of change in absorbance at 410 nm was recorded at 25 °C. A unit of protein is defined as the amount of enzyme required to produce 4-nitroaniline at a rate of 1 μmol/min. The units of active papain at each time point were calculated by using an extinction coefficient for 4-nitroaniline of ε = 8,800 $M^{-1}cm^{-1}$ at 410 nm. In order to determine the possible number of units of active papain in the reaction mixture, enzymatic activity was assessed after a large excess of DTT (~100 fold) was added to an Eppendorf tube. As a control, the addition of DTT was shown to have no bearing on the assay data, other than in activating the enzyme. Y = enzymatic activity (%) at any time point was determined by dividing the number of active units of enzyme by the possible number of units in the solution, and plotted in Fig. 2A. To determine the value of the second-order rate constant (k_{obs}) for the reducing agents, the second order rate equation (eq 4) was transformed into eq 5, which was fitted to the data with the program Prism 5.0. In both equations, A_0 = [inactive protein]$_{t=0}$, A = [inactive protein]$_t$ = $A_0 - A_0Y$, B_0 = [reducing agent]$_{t=0}$, and B = [reducing agent]$_t$ = $B_0 - A_0Y$. Values of k_{obs} (Table S1) are the mean ± SE from three separate experiments.

$$\frac{1}{B_0 - A_0} \ln \frac{A_0 B}{A B_0} = k_{obs} t \tag{4}$$

$$y = \frac{B_0 - B_0 e^{k_{obs} t(A_0 - B_0)}}{B_0 - A_0 e^{k_{obs} t(A_0 - B_0)}} \tag{5}$$

XI. Reactivation of creatine kinase

creatine kinase-Cys283–SH + GSSG → creatine kinase-Cys283–S–S–G + GSH

creatine kinase-Cys283–S–S–G + BMMP (or DTBA or DTT) $\xrightarrow{k_{obs}}$ creatine kinase-Cys283–SH + $BMMP^{ox}$ (or $DTBA^{ox}$ or DTT^{ox})

creatine phosphate + ADP $\xrightarrow{\text{creatine kinase-Cys283–SH}}$ creatine + ATP

ATP + D-glucose $\xrightarrow{\text{hexokinase}}$ ADP + D-glucose-6-phosphate

D-glucose-6-phosphate + $NADP^+$ $\xrightarrow{\text{glucose-6-phosphate dehydrogenase}}$ D-gluconate-6-phosphate + H^+ + **NADPH**

The oxidation and subsequent reactivation of creatine kinase with BMMP (or DTBA or DTT) was accomplished by a procedure described previously.[1,4] Enzymatic activity (%) at particular time points was calculated by dividing the number of active units of enzyme by the possible number of units in solution, and was plotted in Fig. 2B. Values of k_{obs} (Table S1) were determined using eq 5 as described in Section VIII, and are the mean ± SE for three separate experiments.

XII.

Table S1 Values of k_{obs} ($M^{-1}s^{-1}$) for the reduction of disulfides by dithiols

Disulfide	BMMP	DMH	DTBA	DTT
βME^{ox}, pH 7.0	1.02 ± 0.07	0.56 ± 0.04	0.32 ± 0.02	0.090 ± 0.005
βME^{ox}, pH 5.0	0.0183 ± 0.0007	ND[a]	0.0051 ± 0.0004	0.0013 ± 0.0001
papain-Cys25–S–S–CH_3	1139 ± 62	ND[a]	950 ± 51	87 ± 3
creatine kinase-Cys283–S–S–G	476 ± 34	ND[a]	70 ± 2	82 ± 3

[a]ND, not determined.

XIII. Determination of BMMP solubility in buffered water

A 20 mM stock solution of 2-butyne-1,4-diol (which is an ^{1}H NMR standard) was prepared in 50 mM potassium phosphate buffer, pH 7.0. BMMP was added to a solution containing 1 mL of this buffer and 0.1 mL of D_2O until the solution was saturated completely. The mixture was sonicated to ensure complete dissolution and filtered into an NMR tube, and its spectrum was acquired with water suppression. The solubility of BMMP was determined to be (64 ± 14) mM by integration of the ^{1}H NMR peak areas for the aryl C**H** and methylene C$\mathbf{H_2}$SH protons for BMMP and the C$\mathbf{H_2}$OH protons of 2-butyne-1,4-diol. Analogously, the solubility of $BMMP^{ox}$ was determined to be (7.9 ± 2.8) mM by integration of the ^{1}H NMR peak areas for the aryl C**H** protons of $BMMP^{ox}$ and the C$\mathbf{H_2}$OH protons of 2-butyne-1,4-diol.

XIV. NMR Spectra

^{1}H NMR ($CDCl_3$) and ^{13}C NMR ($CDCl_3$) of **3**

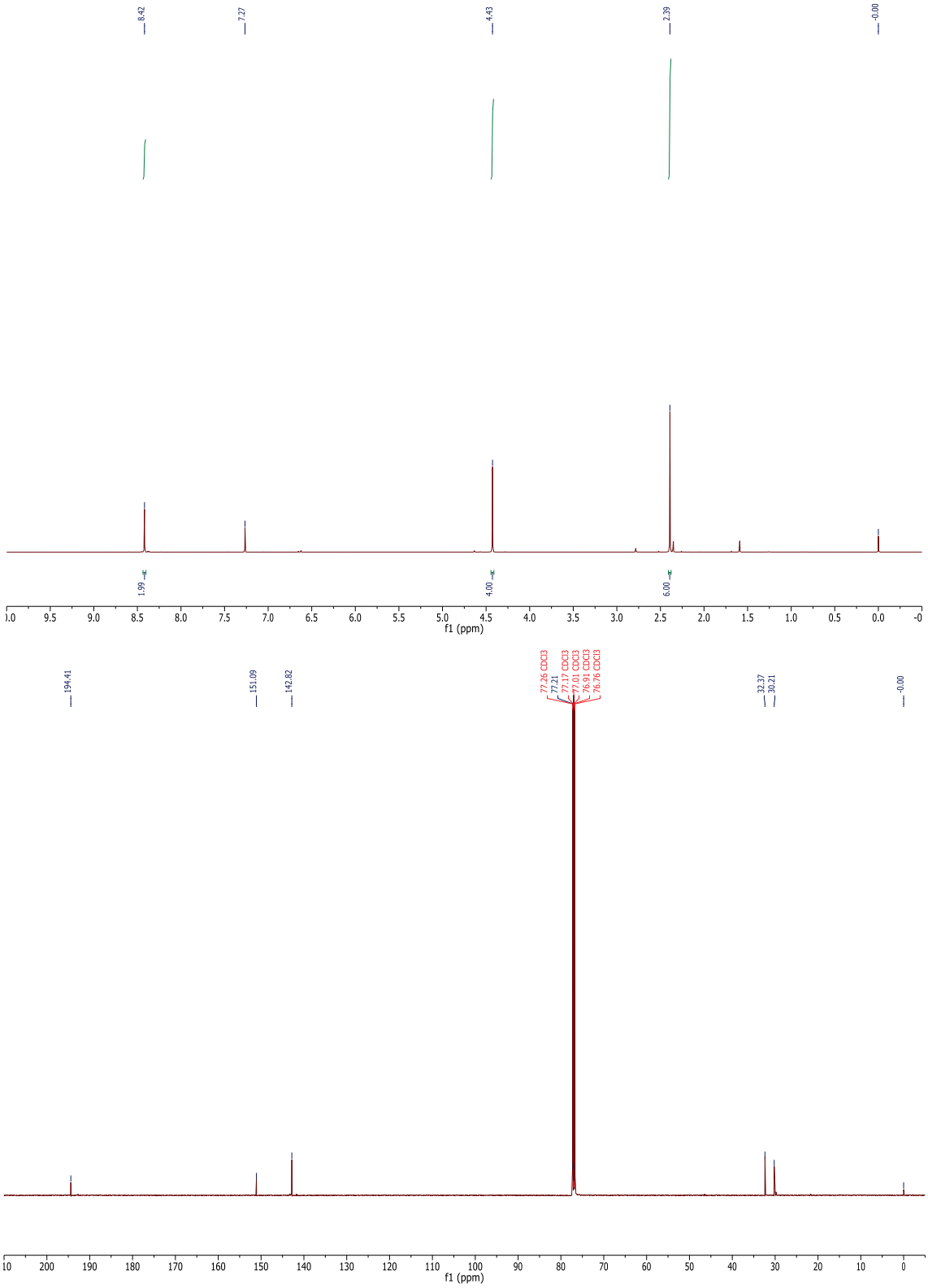

^{1}H NMR (DMSO-d_6) and ^{13}C NMR (DMSO-d_6) of **4** (BMMP)

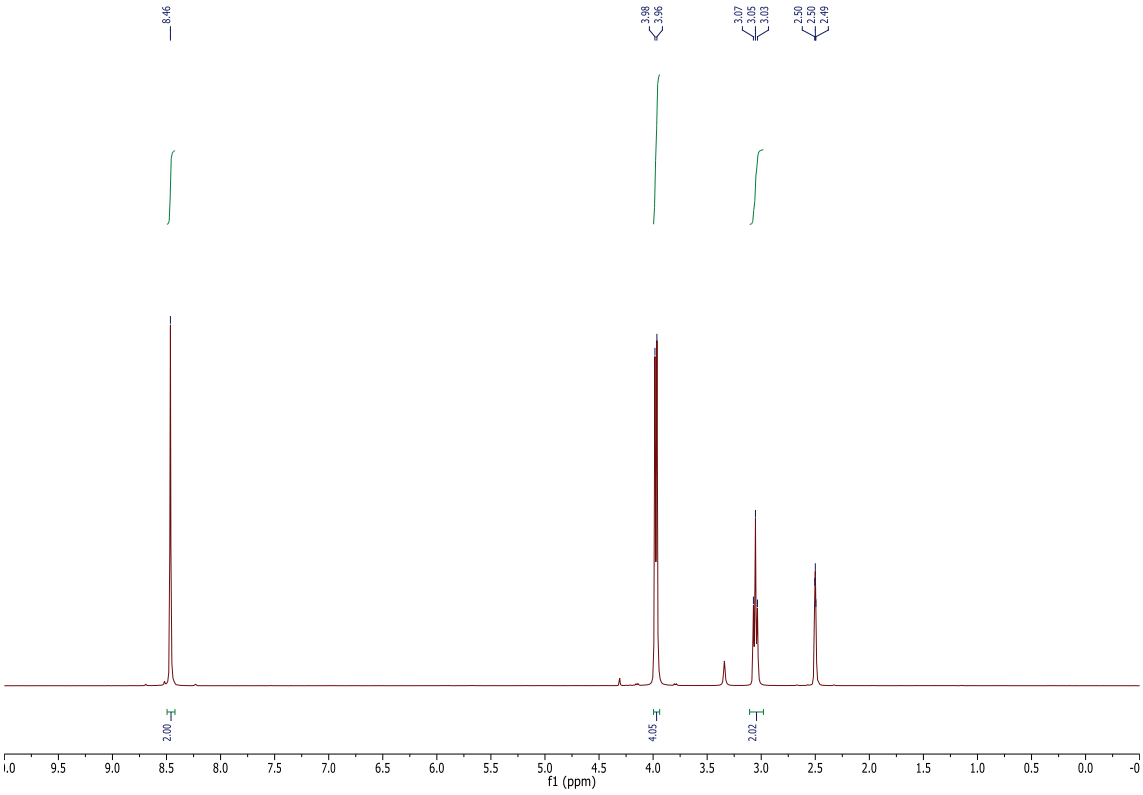

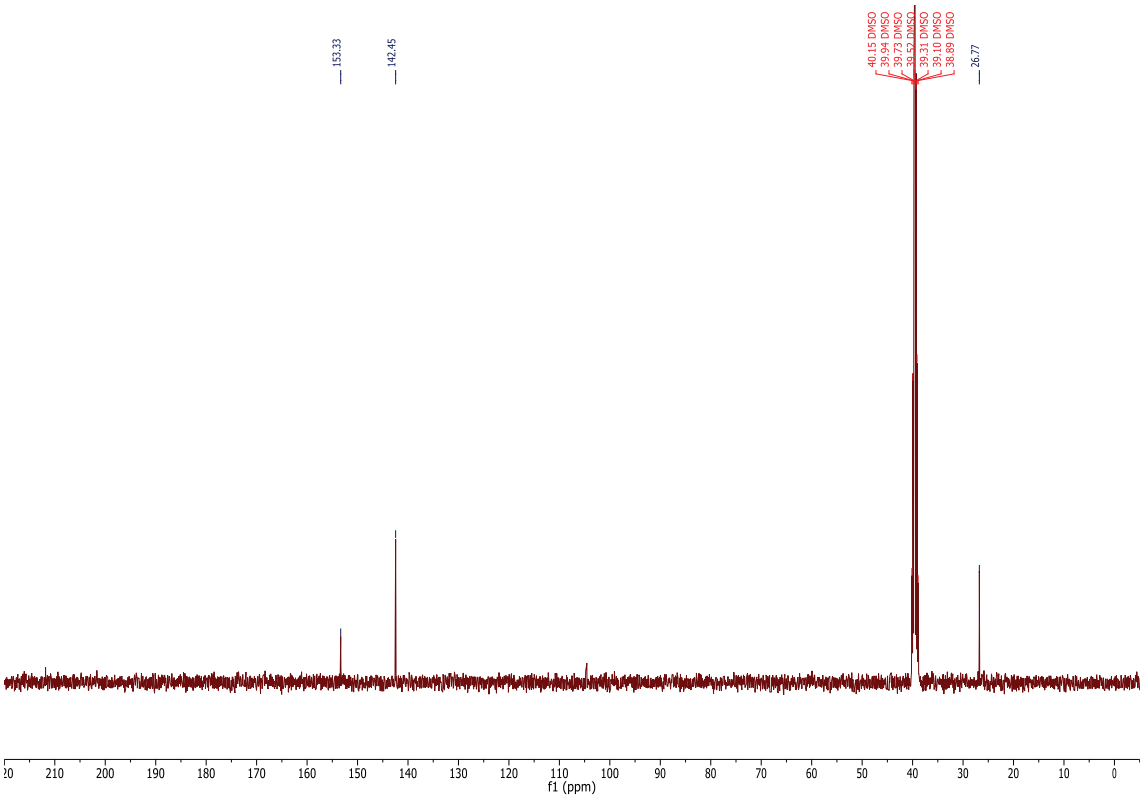

^{1}H NMR ($CDCl_3$) and ^{13}C NMR ($CDCl_3$) of **5** ($BMMP^{ox}$)

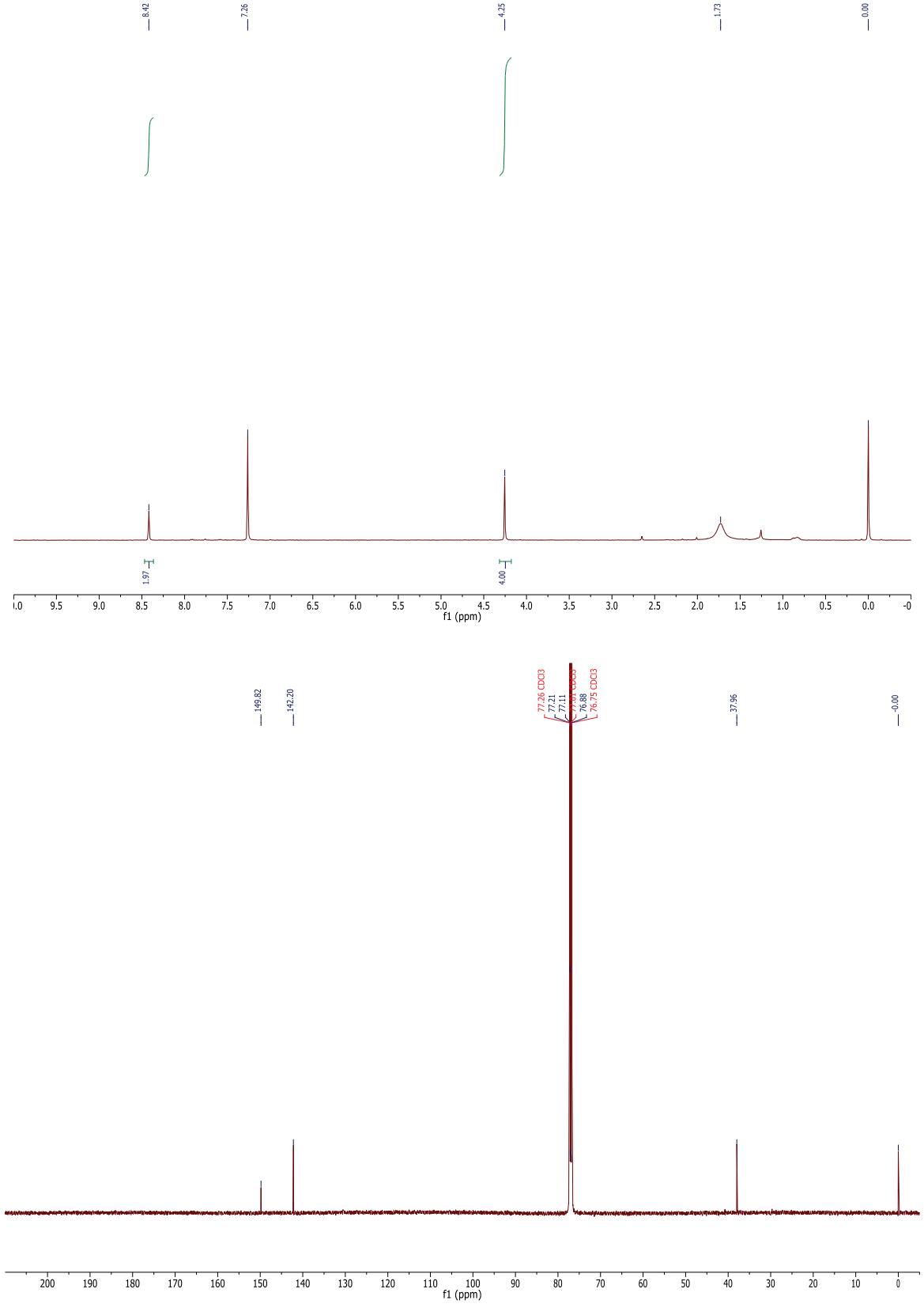

^{1}H NMR (Methanol-d_4) and ^{13}C NMR (Methanol-d_4) of **6** (DMH)

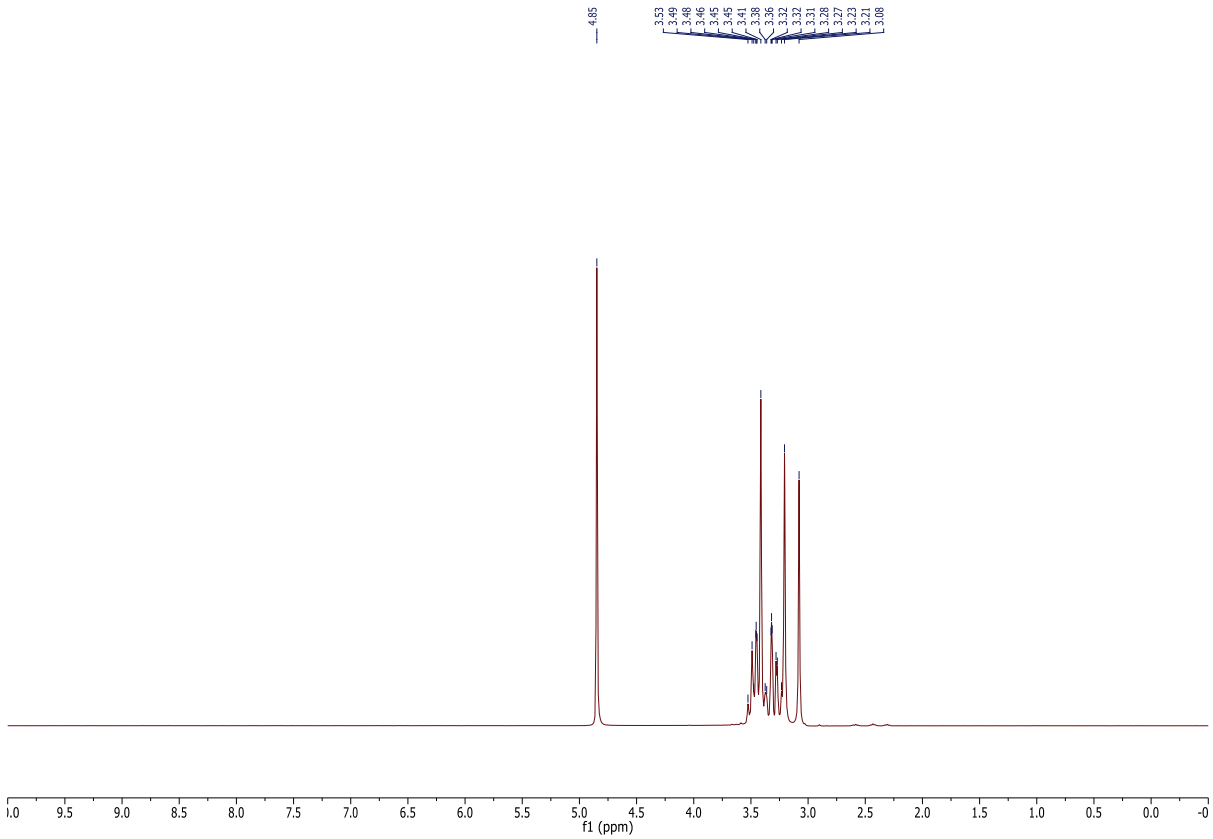

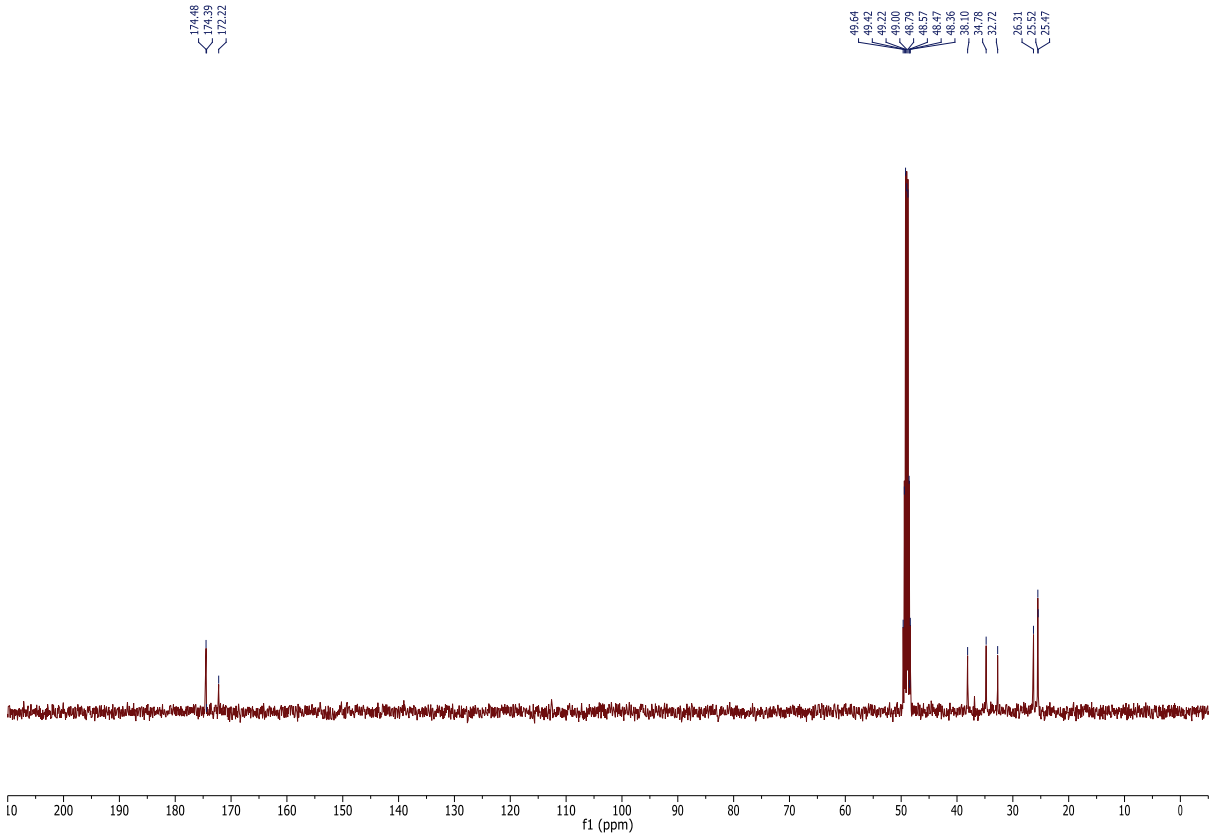

^{1}H NMR (50 mM potassium phosphate buffer, pH 7.0)

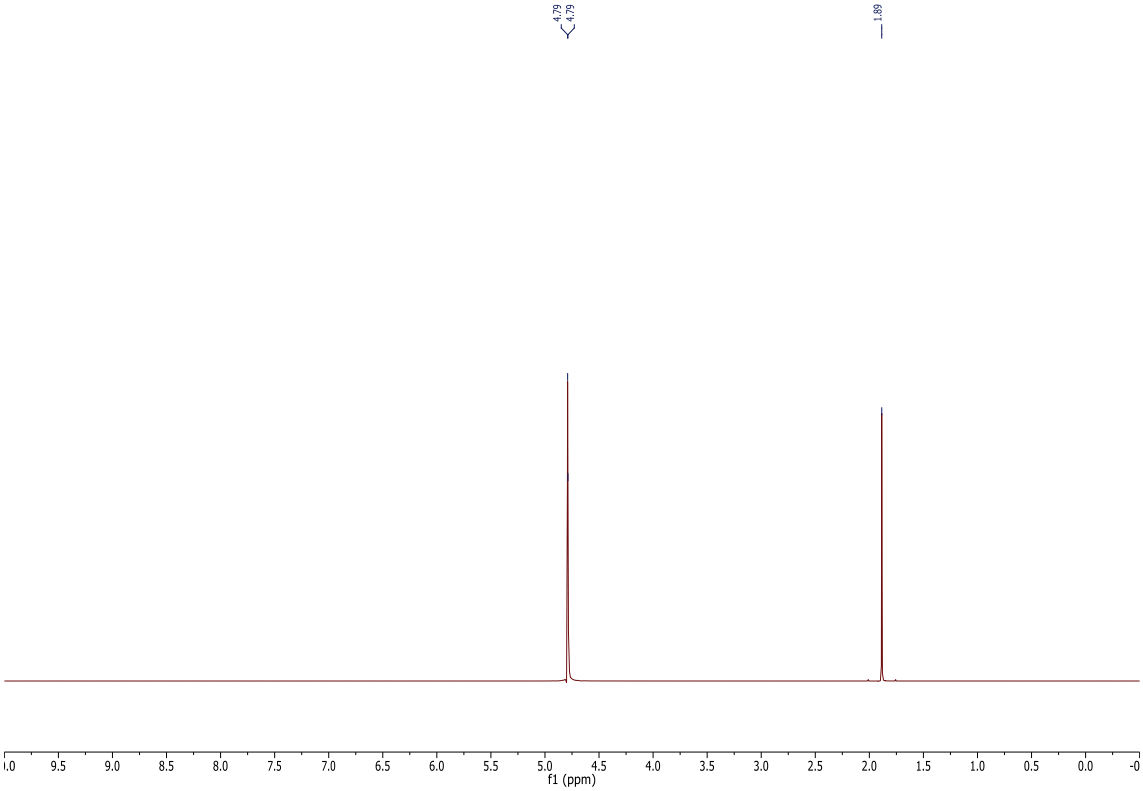

^{1}H NMR (50 mM phosphate buffer, pH 7.0) of **4** (BMMP)

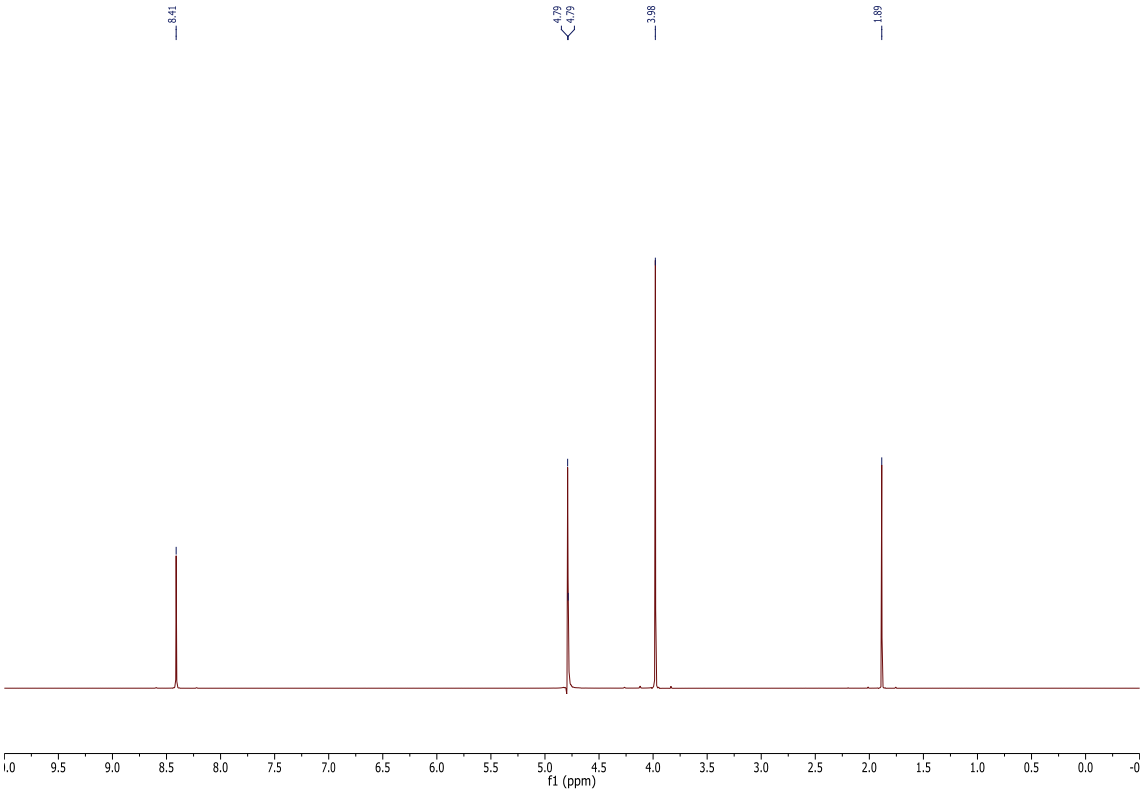

^{1}H NMR (50 mM potassium phosphate buffer, pH 7.0) of 2-butyne-1,4-diol

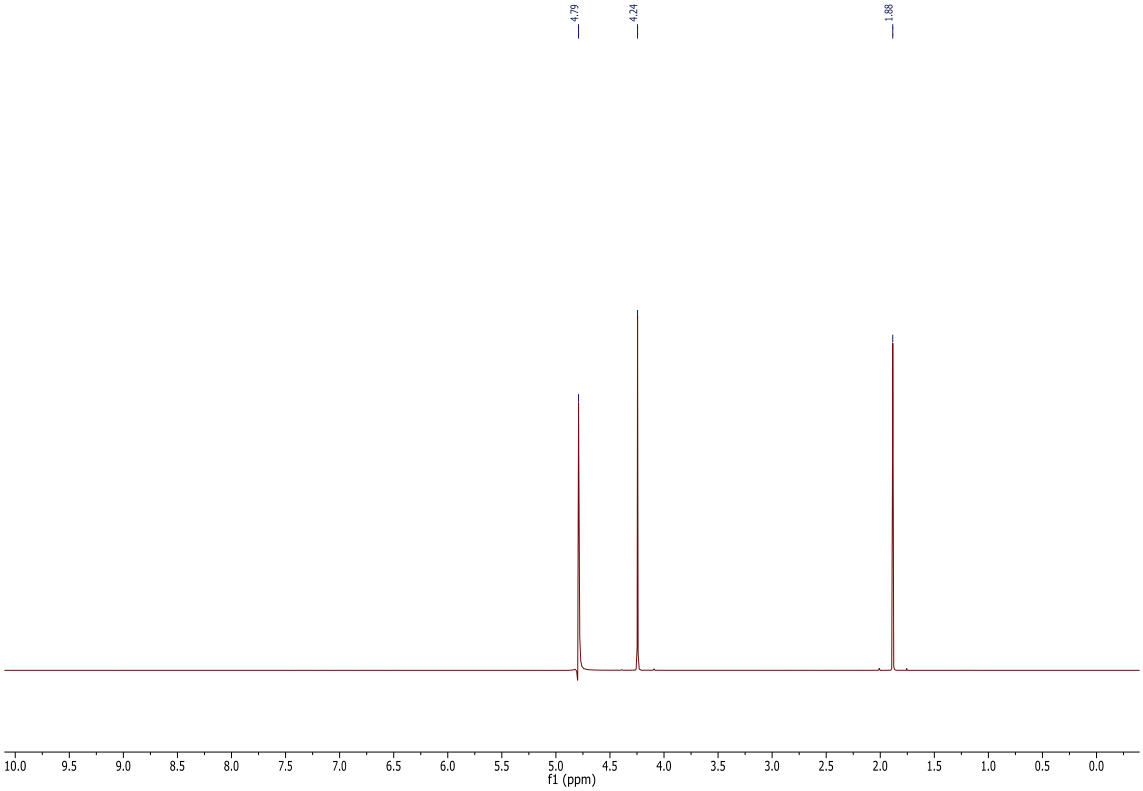

^{1}H NMR (50 mM potassium phosphate buffer, pH 7.0, 20 mM 2-butyne-1,4-diol) of **4** (BMMP)

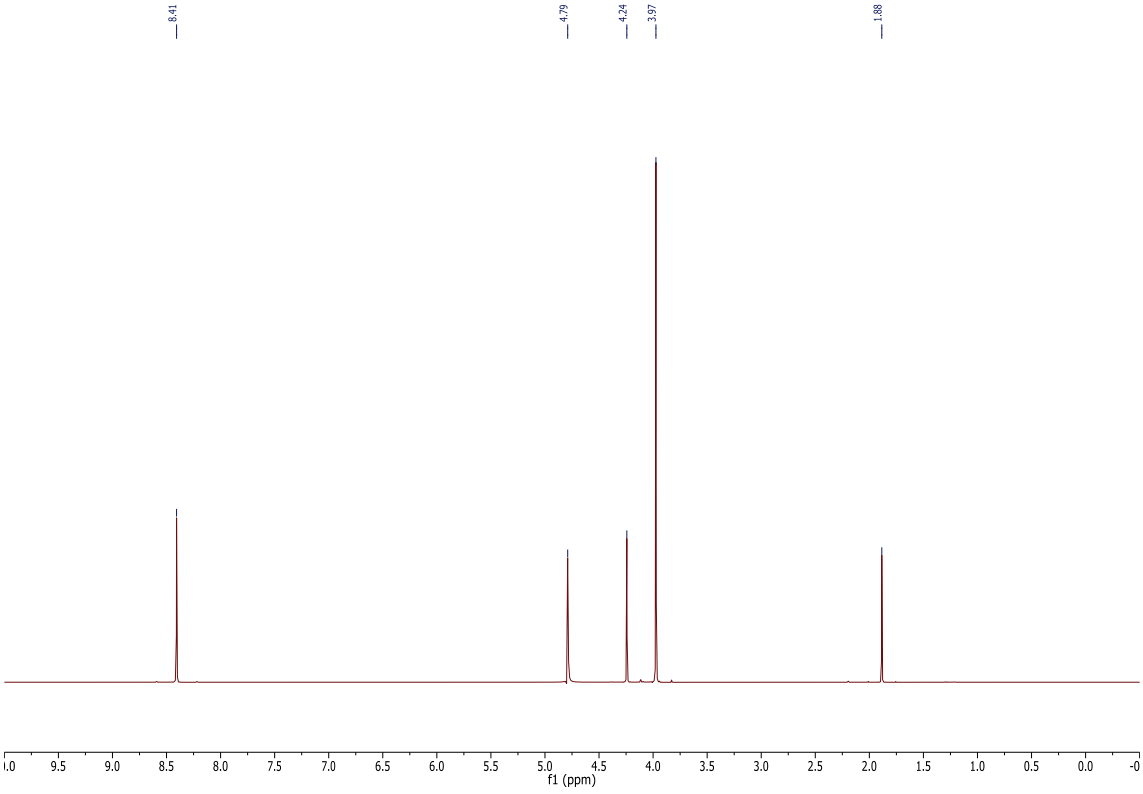

^{1}H NMR (50 mM potassium phosphate buffer, pH 7.0, 20 mM 2-butyne-1,4-diol) of **5** (BMMP^{ox})

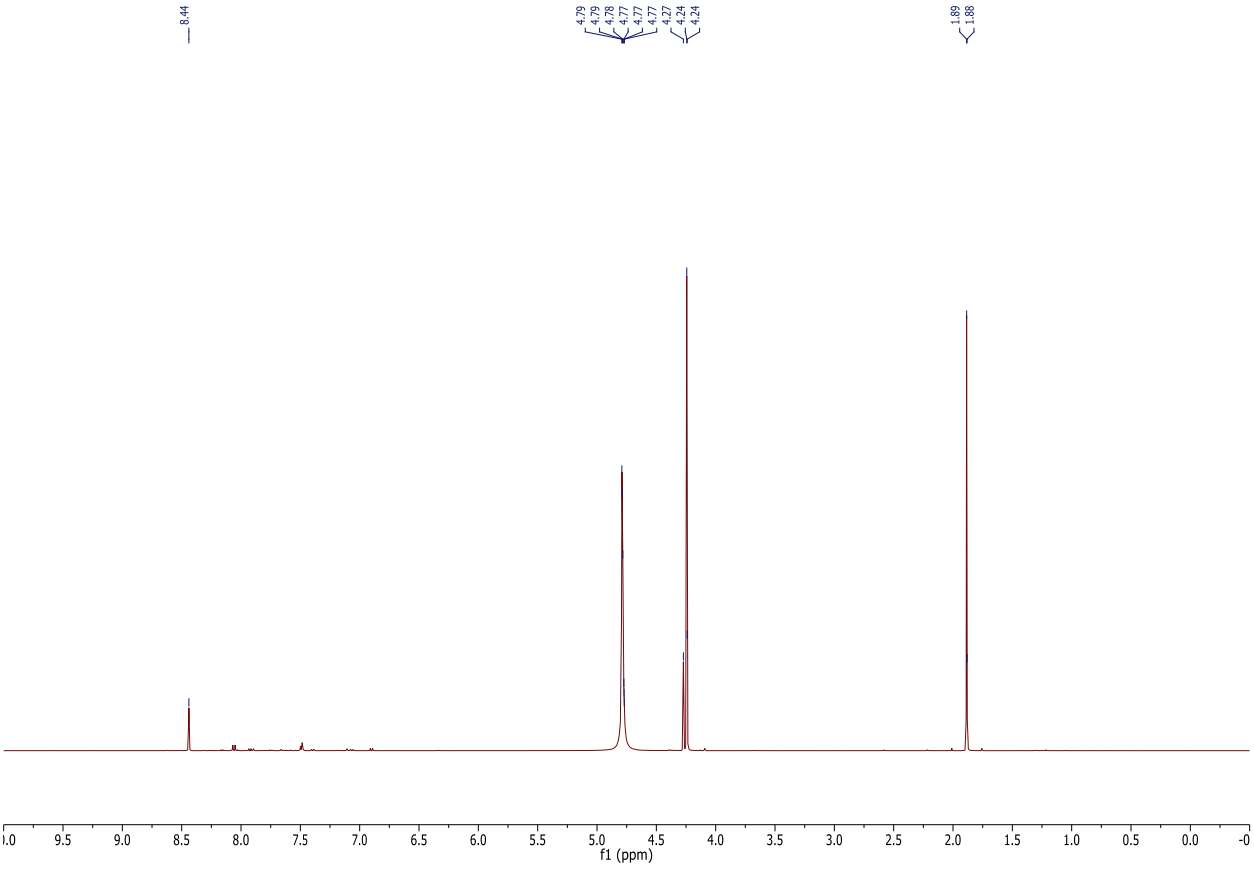

XV. Cartesian coordinates of optimized geometries and partial atomic charges

Table S2 Cartesian coordinates of the optimized geometry of **4** (reduced BMMP); free energy = −1139.389339 Hartree

C	0.00000000	0.00000000	0.00000000
C	-0.95406700	1.07250700	-0.43806000
C	-2.32291100	0.83373200	-0.69034200
N	-3.12240600	1.82086200	-1.07841100
C	-2.59182700	3.03476500	-1.22931700
C	-1.24773000	3.26835200	-0.98751200
N	-0.43413900	2.28972000	-0.58931400
H	-0.81443200	4.25535900	-1.10974500
H	-3.25696800	3.83042800	-1.54751800
C	-2.92142600	-0.53899100	-0.53051100
S	-4.70572000	-0.53774300	-0.98365800
H	-4.85263500	-1.85935000	-0.77304500
H	-2.81760500	-0.87090500	0.50515100
H	-2.38599000	-1.24556300	-1.16673800
S	0.66126500	-0.99964900	-1.41064300
H	1.21766000	0.03512700	-2.06358900
H	-0.47442700	-0.73372000	0.65100300
H	0.83323800	0.45281700	0.53183300

Table S3 Partial atomic charges for the optimized geometry of **4** (reduced BMMP)

Atom	Symbol	Charge
1	C	-0.240841
2	C	-0.083063
3	C	0.426888
4	N	-0.162639
5	C	0.154077
6	C	-0.023234
7	N	-0.235077
8	H	0.106517
9	H	0.108367
10	C	-0.415207
11	S	-0.196545
12	H	0.081154
13	H	0.148652
14	H	0.170850
15	S	-0.228549
16	H	0.100887
17	H	0.127196
18	H	0.160566

Table S4 Cartesian coordinates of the optimized geometry of **5** (oxidized BMMP); free energy = –1138.202460 Hartree

C	0.00000000	0.00000000	0.00000000
C	-1.22554800	-0.87538800	-0.15546100
C	-1.22555800	-2.26904600	-0.35947600
C	-0.00002400	-3.14443300	-0.51498800
S	1.53191200	-2.49364100	0.23405500
S	1.53184400	-0.65070700	-0.74924900
H	0.18165600	-3.34186200	-1.57335300
H	-0.19950400	-4.10073500	-0.02744000
N	-2.37735100	-2.93831700	-0.46398300
C	-3.51420300	-2.25834300	-0.36282000
C	-3.51419100	-0.88601700	-0.15237200
N	-2.37733100	-0.20608000	-0.05106000
H	-4.43949200	-0.32573000	-0.06635800
H	-4.43950400	-2.81857800	-0.44914200
H	-0.19959200	0.95635400	-0.48738200
H	0.18177500	0.19727100	1.05838800

Table S5 Partial atomic charges for the optimized geometry of **5** (oxidized BMMP)

Atom	Symbol	Charge
1	C	0.099860
2	C	-0.167780
3	C	-0.167818
4	C	0.099972
5	S	-0.127191
6	S	-0.127156
7	H	0.164104
8	H	0.154199
9	N	-0.262844
10	C	0.032538
11	C	0.032545
12	N	-0.262836
13	H	0.107054
14	H	0.107055
15	H	0.154197
16	H	0.164102

Table S6 Cartesian coordinates of the optimized geometry of reduced DTT; free energy = −1105.325241 Hartree

C	0.00000000	0.00000000	0.00000000
C	-0.79402300	1.30104000	0.06769800
C	-2.30162000	1.13626200	-0.18710600
C	-3.00517800	0.22179600	0.81756800
S	-4.77481800	-0.05831400	0.41201300
H	-5.08077300	1.24065700	0.25394900
H	-2.56374400	-0.77579400	0.80977900
H	-2.91582500	0.62200000	1.82705900
O	-2.90366500	2.42683400	-0.20996900
H	-2.56455600	2.90775200	0.55788500
H	-2.43733400	0.73018600	-1.19243400
O	-0.66699200	1.93945400	1.33999000
H	0.24404300	2.24628600	1.42931100
H	-0.42242700	1.97480000	-0.71341700
S	1.81259900	0.25781000	0.23695700
H	1.82895600	0.09307300	1.56982000
H	-0.10598400	-0.45292300	-0.98725300
H	-0.33447400	-0.72186200	0.74218100

Table S7 Partial atomic charges for the optimized geometry of reduced DTT

Atom	Symbol	Charge
1	C	-0.159791
2	C	0.169594
3	C	0.004885
4	C	-0.000413
5	S	-0.351191
6	H	0.114166
7	H	0.120412
8	H	0.155895
9	O	-0.430165
10	H	0.270291
11	H	0.114107
12	O	-0.483914
13	H	0.281039
14	H	0.114165
15	S	-0.320047
16	H	0.103947
17	H	0.150258
18	H	0.146763

Table S8. Cartesian coordinates of the optimized geometry of oxidized DTT. Free Energy = −1104.138109 Hartree

C	0.00000000	0.00000000	0.00000000
S	1.58410300	-0.59440700	0.69404000
S	1.55983500	-2.53693800	-0.08696400
C	-0.03960000	-3.08756600	0.61824800
C	-1.21551300	-2.26174400	0.09301900
C	-1.19874700	-0.78897800	0.51946200
H	-1.19783400	-0.75674700	1.61707900
O	-2.35428100	-0.12919000	0.01488200
H	-3.11187900	-0.69176200	0.22379600
H	-1.23177900	-2.30038500	-1.00189100
O	-2.45056800	-2.77838400	0.61772400
H	-2.68506300	-3.58556300	0.14759400
H	-0.14886400	-4.13017700	0.30556300
H	0.00642400	-3.05617000	1.70707400
H	0.04305300	-0.02076000	-1.08909600
H	-0.09487400	1.03891800	0.32344100

Table S9. Partial atomic charges for the optimized geometry of oxidized DTT**.**

Atom	Symbol	Charge
1	C	0.004557
2	S	-0.114737
3	S	-0.116856
4	C	-0.050649
5	C	-0.167983
6	C	-0.010352
7	H	0.106491
8	O	-0.445927
9	H	0.289631
10	H	0.117979
11	O	-0.462627
12	H	0.275991
13	H	0.123442
14	H	0.155189
15	H	0.149212
16	H	0.146639

Table S10. Cartesian coordinates of the optimized geometry of DMH. Free Energy = −1292.247888 Hartree

C	0.00000000	0.00000000	0.00000000
N	-0.09508500	-0.72761800	1.26396700
N	-1.36704900	-0.72553300	1.84557400
C	-1.44858400	-0.08410700	3.15535000
H	-0.93251100	0.87414100	3.10212800
H	-2.48801000	0.10661100	3.41188700
H	-0.98484700	-0.70079500	3.92838800
C	-2.25122700	-1.67697500	1.36582200
C	-3.55785300	-1.81976500	2.12936700
S	-4.63902300	-2.99109900	1.21888200
H	-5.66298900	-2.86955300	2.08385400
H	-3.34861000	-2.20054400	3.13049200
H	-4.05286800	-0.85267800	2.22149300
O	-2.00547600	-2.33199900	0.37369700
C	0.75646800	-1.73425000	1.68193100
C	2.05900800	-1.87269900	0.89913800
S	3.29880600	-2.92339300	1.74004900
H	2.39446400	-3.55250200	2.51311500
H	1.81925700	-2.29054900	-0.08149500
H	2.52174500	-0.89920900	0.74327100
O	0.47129700	-2.44906400	2.62230000
H	1.04186600	0.15213500	-0.26880700
H	-0.51090200	-0.53796500	-0.80119700

H	-0.46271400	0.97795100	0.13063100

Table S11. Partial atomic charges for the optimized geometry of DMH**.**

Atom	Symbol	Charge
1	C	-0.283588
2	N	-0.028313
3	N	-0.002310
4	C	-0.287588
5	H	0.136125
6	H	0.131272
7	H	0.175265
8	C	0.240271
9	C	-0.091617
10	S	-0.224413
11	H	0.083872
12	H	0.159114
13	H	0.144822
14	O	-0.434543
15	C	0.206672
16	C	-0.031179
17	S	-0.308059
18	H	0.132124
19	H	0.168848
20	H	0.135352
21	O	-0.463912
22	H	0.128362
23	H	0.178108
24	H	0.135314

Table S12. Cartesian coordinates of the optimized geometry of oxidized DMH. Free Energy = −1291.051740 Hartree

C	0.00000000	0.00000000	0.00000000
S	-0.78787300	-1.69121900	-0.04339800
S	0.46337800	-2.91302600	1.08652400

C	1.89945700	-3.27718600	-0.01717500
C	3.27024000	-2.59799100	0.11909100
N	3.39844600	-1.28041600	0.50354300
N	2.27540200	-0.49909200	0.73704600
C	1.45879300	-0.20879800	-0.34031700
O	1.84108000	-0.30980500	-1.48968300
C	2.06345600	-0.09614500	2.12630500
H	1.45238500	0.80254500	2.16717300
H	1.59473600	-0.88982400	2.71072400
H	3.03187000	0.14598100	2.56449800
C	4.66927600	-0.58386100	0.31361500
H	4.82008100	0.12533900	1.12841100
H	5.46720900	-1.32023500	0.32085600
H	4.66827200	-0.05089700	-0.63952700
O	4.24845000	-3.25556100	-0.18285300
H	2.10181700	-4.34007400	0.10741600
H	1.56379400	-3.12250600	-1.04432600
H	-0.48608500	0.54280400	-0.80862800
H	-0.20314300	0.47491800	0.95448900

Table S13. Partial atomic charges for the optimized geometry of oxidized DMH**.**

Atom	Symbol	Charge
1	C	-0.307967
2	S	-0.122816
3	S	0.130840
4	C	-0.193910
5	C	0.211784
6	N	0.059248
7	N	-0.203296
8	C	0.334650
9	O	-0.404489
10	C	-0.350976
11	H	0.133997
12	H	0.172818
13	H	0.141434
14	C	-0.269997
15	H	0.117610
16	H	0.175912
17	H	0.153596
18	O	-0.464211
19	H	0.178585

20	H	0.201215
21	H	0.175584
22	H	0.130389

XVI. References

1. J. C. Lukesh, M. J. Palte and R. T. Raines, *J Am Chem Soc*, 2012, **134**, 4057–4059.
2. M. J. T. Frisch, G. W.; Schlegel, H. B.; Scuseria, G. E.; Robb, M. A.; Cheeseman, J. R.; Scalmani, G.; Barone, V.; Mennucci, B.; Petersson, G. A.; Nakatsuji, H.; Caricato, M.; Li, X.; Hratchian, H. P.; Izmaylov, A. F.; Bloino, J.; Zheng, G.; Sonnenberg, J. L.; Hada, M.; Ehara, M.; Toyota, K.; Fukuda, R.; Hasegawa, J.; Ishida, M.; Nakajima, T.; Honda, Y.; Kitao, O.; Nakai, H.; Vreven, T.; Montgomery, Jr., J. A.; Peralta, J. E.; Ogliaro, F.; Bearpark, M.; Heyd, J. J.; Brothers, E.; Kudin, K. N.; Staroverov, V. N.; Kobayashi, R.; Normand, J.; Raghavachari, K.; Rendell, A.; Burant, J. C.; Iyengar, S. S.; Tomasi, J.; Cossi, M.; Rega, N.; Millam, J. M.; Klene, M.; Knox, J. E.; Cross, J. B.; Bakken, V.; Adamo, C.; Jaramillo, J.; Gomperts, R.; Stratmann, R. E.; Yazyev, O.; Austin, A. J.; Cammi, R.; Pomelli, C.; Ochterski, J. W.; Martin, R. L.; Morokuma, K.; Zakrzewski, V. G.; Voth, G. A.; Salvador, P.; Dannenberg, J. J.; Dapprich, S.; Daniels, A. D.; Farkas, Ö.; Foresman, J. B.; Ortiz, J. V.; Cioslowski, J.; Fox, D. J. , Gaussian, Inc., Wallingford, CT, 2009.
3. J. H. Liu, A. T. Wu, M. H. Huang, C. W. Wu and W. S. Chung, *J. Org. Chem.*, 2000, **65**, 3395–3403.
4. R. Singh and G. M. Whitesides, *J. Org. Chem.*, 1991, **56**, 2332–2337.
5. K. J. Woycechowsky, K. D. Wittrup and R. T. Raines, *Chem. Biol.*, 1999, **6**, 871–879.
6. R. E. Benesch and R. Benesch, *J Am Chem Soc*, 1955, **77**, 5877–5881.
7. G. V. Lamoureux and G. M. Whitesides, *J. Org. Chem.*, 1993, **58**, 633–641.
8. G. L. Kenyon, *Biochemistry*, 1975, **14**, 766–771.